

The influence of Chromium concentration on the corrosion resistance of the electrodeposited Zn–Co–Cr alloys

L.Tahraoui, M. Diafi*, A. Fadel

Department of Chemical Industry, University of Biskra, Algeria

Electrodeposition operating conditions for Zn–Co–Cr alloys from sulfate baths and the corrosion resistance of the electrodeposited alloys were studied. The effects the concentration of cobalt on zinc-cobalt alloys obtained from sulphate baths under continuous current deposition are described. The deposit morphology was analyzed using Scanning Electron Microscopy (SEM) and an X-Ray Diffraction (XRD) was used to determine the preferred crystallographic orientations of the deposits. Protection against corrosion properties studied in a solution of 3,5 % wt NaCl in the potentiodynamic polarization measurements (Tafel), electrochemical impedance spectroscopy (EIS) to the potential of corrosion free. The parameters that characterize the corrosion behavior can be determined from the plots and Nyquist plots. X-ray diffraction studies of the deposit showed the presence of Co₅Zn₂₁ phase and η - phase. The obtained data also exposed that the corrosion resistance increases as a result of increasing Cr concentration and the addition of Cr in the Zn-Co increases the micro-hardness

(Received January 13, 2021; Accepted April 27, 2021)

Keywords: Zn–Co alloys, Zn-Co-Cr alloy, XRD, Microhardness, Electrodeposition, Corrosion resistance

1. Introduction

Considerable research has been performed to improve the corrosion resistance of metallic surfaces. Zinc coatings are used widely to protect iron and steel substrates against corrosion [1]. Electroplated binary Zn-Malloys, where metals are a Fe group such as Fe, Co, Sn, Ni, Mn and Cr [2] Electrodeposited zinc has been widely used in a variety of applications, including coatings for automotive and electronic parts [3]. The electrodeposition of zinc–cobalt alloys is of great interest because these alloys exhibit significantly higher corrosion resistance than pure zinc [4]. It sensed that it will be important to accumulate the Zn-Co binary alloys properties in one alloy through the electroplating of Zn-Co-Cr ternary alloy. The first aim of our study is to electrodeposite Zn-Co-Cr alloy coatings on two steel substrates with useful form in sulphate bath. The second aim is to make a comparison between Zn-Co and Zn-Co-Cr alloys for structural phases, morphology of surface and the resistance of corrosion. The ternary alloys are prepared under similar electrolysis conditions like the Zn–Co binary alloy, the composite coatings have been characterized, morphological (SEM), structural (XRD), and electrochemical properties of the composite coatings have been studied by potentiodynamic polarization and electrochemical impedance spectroscopy in a solution of 3,5 % NaCl.

2. Experimental

2.1. Coating processes

The electroplating of Zn-Co coatings was carried out on steel substrates, under conditions at the operating current density of 25 A cm⁻² and a temperature of 25°C. The chemical composition of the used bath is given in Table 1 [5, 6]. Electrodeposits Zn-Co were obtained by varying the Chromium sulfate concentration (CrSO₄·7H₂O) in the bath (0, 10, 15, 20 g·L⁻¹).

*Corresponding author: m.diafi@univ-biskra.dz

Table 1. Solution composition and conditions for alloy electroplating.

Electrolyte I	Concentration (g·l ⁻¹)	Plating parameters
ZnSO ₄ ·7H ₂ O	57.5	25°C and pH=3,5 constant current densities at 25 mA cm ⁻² for 60s
CoSO ₄	52.5	
H ₃ BO ₃	9.3	
Na ₂ SO ₄	56.8	
Na ₃ C ₆ H ₅ O ₇	56.8	

2.2. Coating characterization

The phase structure of the coatings was determined using X-ray diffraction with a D8 Advance-Brucker using a Cu K α radiation ($\lambda = 1.5406 \text{ \AA}$) and 0.02° as 2θ step.

Scherrer's formula is used for the determination of the coatings crystallite sizes from the X-ray peak broadening of the (101) diffraction peak at [7]:

$$D = \frac{0.9\lambda}{\beta \cos\theta} \quad (1)$$

where D is the grain size, λ is the X-ray wavelength, β is the corrected peak full width at half-maximum intensity (FWHM), and θ is Bragg angle position of the considered peak.

The deposits surface morphology was studied by scanning electron microscopy (A JEOL model JSM6390LV).

Microhardness of coatings was measured using a load of 100 g with a holding time of 15s by using a Vickers hardness tester, and the average of ten hardness measurements was quoted as the hardness value.

The corrosion behavior and the protection performance of Zn-Co alloy and Zn-Co-Cr composite coatings were studied by using electrochemical impedance spectroscopy (EIS) and electrochemical Tafel extrapolation (TE) in 3,5 % wt NaCl solution. The tests were performed using a potentiostat galvanostat (a Volta Lab 40 model). A coated sample was served as a working electrode, the counter electrode was platinum with a surface of 1 cm² and the Hg/HgO/ 1 M KOH is used as a reference electrode. The impedance data were obtained at open-circuit potential and the measurements were carried out over a frequency range of 10 kHz- 50 MHz using the amplitude of sinusoidal voltage (10mV). Potentiodynamic polarization with a scan rate of 50mV/s was applied in order to study the anodic dissolution of the coatings. The corrosion current density (I_{corr}) and corrosion potential (E_{corr}) were determined using TE.

3. Results and discussions

3.1. X-ray diffraction

XRD patterns for the "as-deposited" Zn-Co and Zn-Co-Cr alloy coatings are presented in Fig.1. The Zn-Co alloy coatings have the same structure as zinc deposits [8]. The metallic phases are well crystalline and can be ascribed to the zinc-rich (η -phase) hexagonal structure and cubic Co₅Zn₂₁ phases. Adding Chromium atoms in the zinc-cobalt alloy shifted towards more big reflection angles for all the η phases. A decrease of (101) peak was observed when the Chromium level in the film was increased. The decrease of this peak may be attributed to the decrease of the zinc content in the coating. No Cr phase was observed [9].

Crystallite sizes were determined using the Scherrer formula. For all coatings, the profile of (101) peak exhibits Lorentzian line shape, with an increase in Cr content grain sizes decrease in a regular way (Table 2) [10].

Table 2. Values of the crystallite size obtained from the strongest diffraction line of the metallic phases.

Electrolyte	hkl	2 θ ($^{\circ}$)	Crystal size (nm)
Zn-Co (0 g /l Cr)	(101)	43.15	58,8
Zn-Co-Cr (10 g /l Cr)	(101)	43.18	50
Zn-Co-Cr (15 g /l Cr)	(101)	43.28	41,53
Zn-Co-Cr (20 g /l Cr)	(101)	43.39	36,36

3.2. Surface morphology

The morphology of these coatings plated in different compositions and for two magnifications (20 and 30 μ m is presented in Fig. 2(a-d).Which indicates the complete coating,compact and homogeneous deposits on the substrate surface [11]

3.3. EDX analysis of the Zn-Co- Cr composite coating

Fig.3 showed the variation (EDX) results of various developed deposits, which confirmed that the Zinc is the metal matrix, while Cobalt and Chromium are co-deposited with the metal matrix. The rate of Cr co-deposition reaches the maximum value (1,94wt% at 20 g \cdot l $^{-1}$ (Fig.3 .b).

Table 3. Values of micro-hardness Vickers hardness (HV) registered different electro deposition.

Coating	hardness
Zn-Co	177.8
Zn-Co-Cr (10 g /l)	268,4
Zn-Co-Cr (15 g /l)	395
Zn-Co-Cr (20 g /l)	491,25

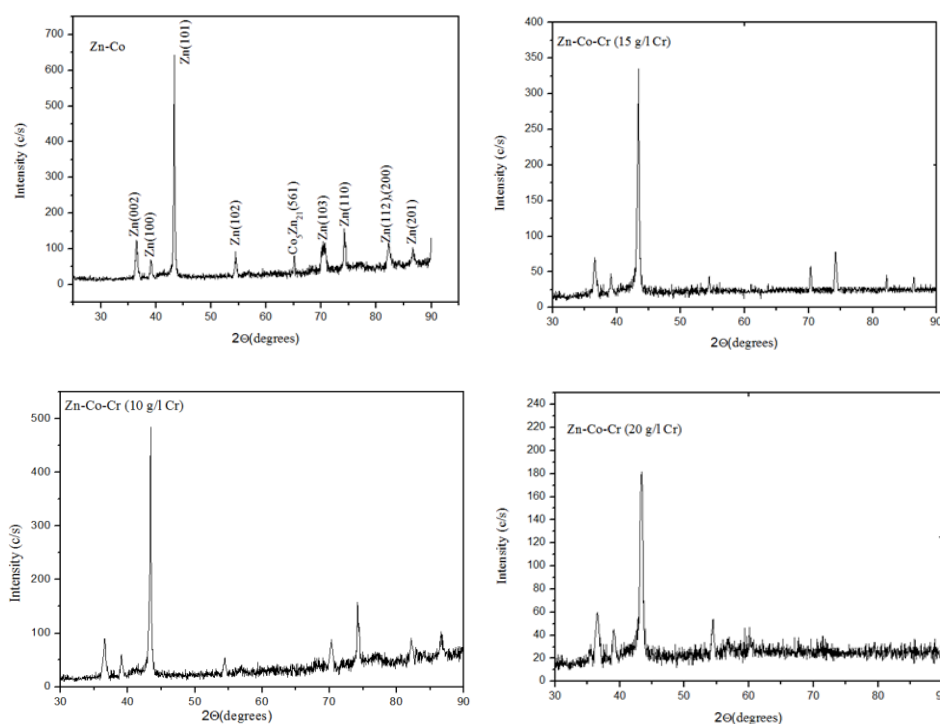


Fig. 1. X-ray diffraction patterns of Zn-Co alloy coatings and Zn-Co-Cr (10 g /l Cr), Zn-Co-Cr (15 g /l Cr), Zn-Co- Cr (20 g /l Cr) Composite coatings deposited at 30 mA.cm $^{-2}$, T = 30 $^{\circ}$ C, and pH = 3-5 for 60s.

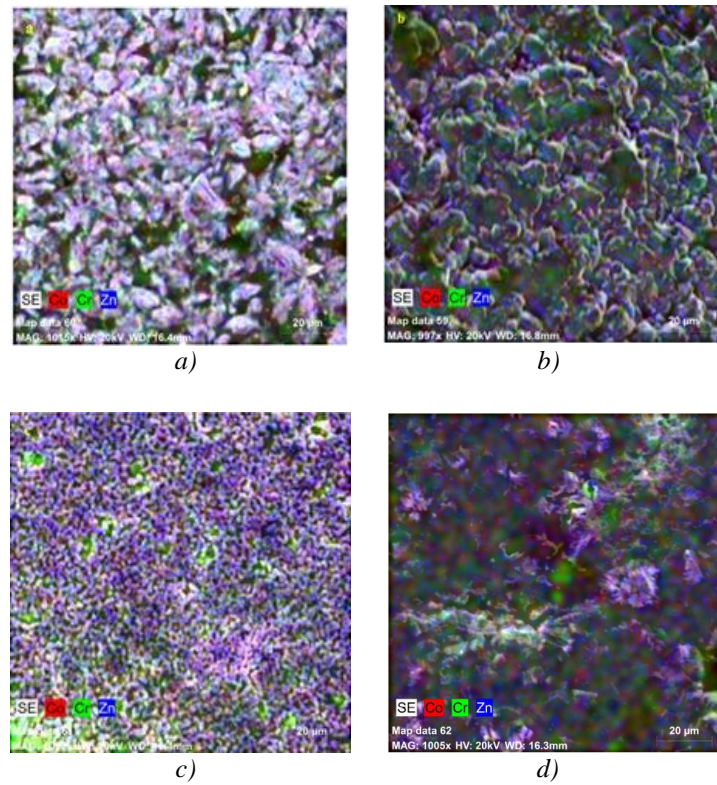


Fig. 2 Surface morphology of (a) Zn-Co alloy coatings and (b) Zn-Co- Cr (10 g /l Cr), (c) Zn-Co- Cr (15 g /l Cr) , (d) Zn-Co-Cr (20 g /l Cr) Composite coatings deposited at 30 mA.cm ⁻² , T = 30 °C, and pH 3-5 for 60s.

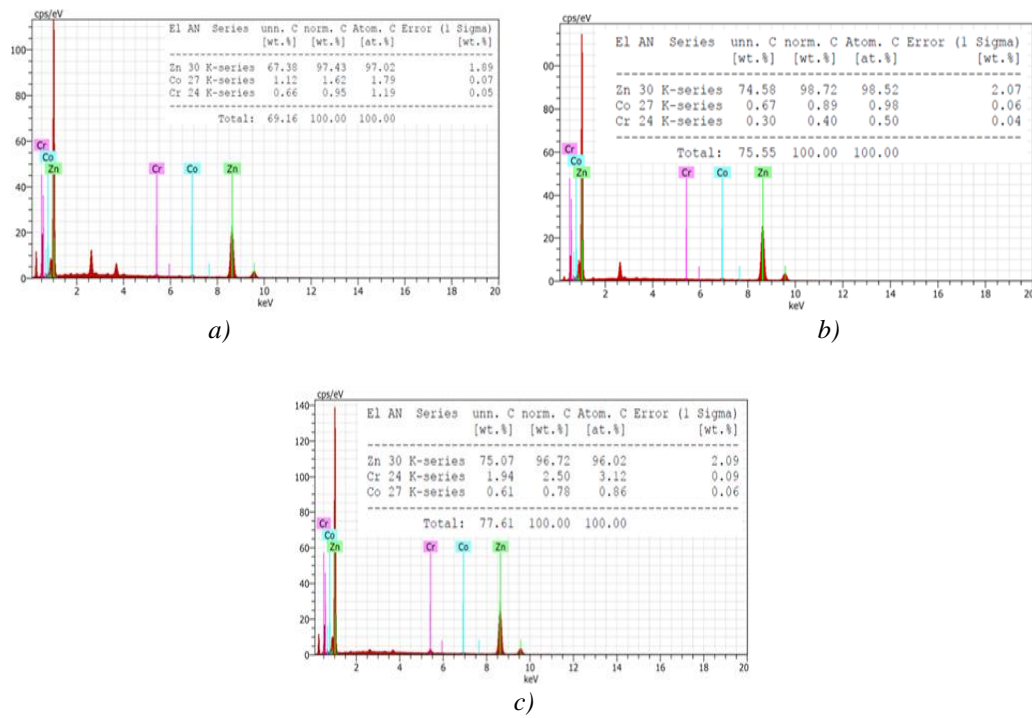


Fig. 3EDAX of Zn-Co-Cr (10 g /l Cr), (b) Zn-Co-Cr (15 g /l Cr) , (c) Zn-Co-Cr (20 g /l Cr) Composite coatings deposited at 30 mA.cm ⁻² , T = 30 °C, and pH 3-5 for 60s.

3.4. Effect of chromium content of the bath on coatings microhardness

The variation of microhardness vs chromium content in the deposited Zn-Co-Cr alloy coatings is shown in Table 2. This figure indicates that the micro hardness of Zn-Co alloy coatings increases with increasing chromium content. This is because that the hardness of Cr is greater than Zn-Co, The hardness increased from 177 Hv for Zn-Co, alloy to 268,4 and 491,25 Hv for 10 g /land 20 g /lCr alloy coating respectively, Hardness values enhance with Co content, it can be correlated to the (i) formation of solid solution, (ii) formation of two phase structure, (iii) grain size effects[12].

3.5. Electrochemical measurements

3.5.1. Potentiodynamic polarization studies

Tafel tests were performed on Zn-Co alloy and Zn-Co-Cr composite coatings in a 3.5 % NaCl solution. Tafel polarization readings have been shown in Fig 4. The corresponding electrochemical parameters extracted from Tafel plots are summarized in Table 3. Results indicated that the corrosion potentials of Zn-Co- Cr composite coatings shift to the positive direction and corrosion current density decreased significantly compared to Zn-Co alloy coatings. The increase of chromium content in the deposits is caused a finer grain size and an increase in corrosion resistance of Zn-Co-Cr alloys. [13 ,14].

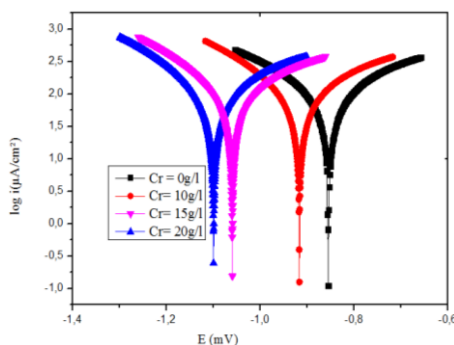


Fig. 4 Polarizing curves obtained for the alloy coatings in a 3.5 % NaCl solution at different concentrations of Cr.

Table 4. Electrochemical parameters of the coatings derived from Tafel plots.

Coating	E_{corr}	i_{corr}	R_p
Zn-Co	-0,855	0,2749	12,04
Zn-Co- Cr (10 g /l)	-0,916	0,4562	49,57
Zn-Co- Cr (15 g /l)	-1,0595	0,646	57,01
Zn-Co- Cr (20 g /l)	-1,0995	0,949	75,86

3.5.2. Electrochemical impedance spectroscopy (EIS) studies

The Nyquist graphs of all the Zn-Co-Cr samples show a single capacitive loop that is not a perfect semicircle, and this is attributed to the dispersion of the frequency of the impedance electrode and electrolyte interface [15,16], usually due to the heterogeneity of the surface of the electrode. This heterogeneity may result from roughness, impurities, dislocations, and formation of porous layers [17,18]. This type of diagram is generally interpreted as a mechanism of charge transfer on a heterogeneous and irregular surface [19,20]. The diameters of capacitive semicircles increase with the increasing concentration of Cr [21-24]. The values of the various parameters of the electrical circuit after modeling. The resistance of the charge transfer increases as a function of the concentration of Cr, and the capacity of the film C_f , calculated from the CPE, and that of the double-layer C_d decrease. The values of C_d are between 8,992 and 0,6155 cm^{-2} , This behavior

corresponds to a capacitor that represents a surface with certain imperfections such as roughness and porosity. For the first resistance R_f , it is attributed to the oxidation reactions of zinc and chromium at the deposition surface, after this oxidation a film of Zn oxides and Cr is formed on the surface. The latter is characterized by its high resistance R_t due to the passive nature of this oxide layer. This indicates that the material transport phenomenon has occurred through the formed oxide layer [25-27]. The results of the Zn-Co-Cr system (0 - 20 g / l), show an increase in the values of the charge transfer resistance R_t , while the capacity of the double layer C_d decreases with respect to the deposition of Zn-Co, which can be explained by the decrease of the active surface in direct contact with the corrosive medium, as a result of the incorporation of the particles, or by the growth of the thickness of the layer of corrosion products. Variations in the strength and capacity values of the double layer, R_t and C_d , suggest the development of the corrosion product layer that forms during long measurement times and increases the corrosion resistance. The impedance results are in agreement with the results extracted from the polarization curves, the best values being observed in the case of Zn-Co-Cr composite deposits, for the concentration of 20 g / l Cr and the lowest of the capacity of the double layer is (0,6155 μ F / cm). Incorporation of Cr Particles Determines Growth of Anti-Corrosion Resistance of Zn-Co deposits

Table 5. Simulation parameters obtained at the abandonment potential.

Coatings	R_e [Ω .cm ²]	R_{ct} [k Ω .cm ²]	C_{dl} [μ F/cm ²]
Zn-Co	4	4,427	8,992
Zn-Co-Cr (10 g / l)	148	4,822	4,307
Zn-Co- Cr (15 g / l)	22	9,000	1,118
Zn-Co- Cr (20 g / l)	3	14,977	0,6155

4. Conclusions

In this study, the effect of Cr contents, in the bath, on structural properties, microhardness and corrosion resistance of Zn-Co alloy coating was investigated. The coatings were deposited on mild steel substrates by electrodeposition from a sulfate bath. Results from this investigation can be drawn as the following points:

XRD and SEM results indicate that Zn-Co alloy coating Zn-Co-Cr composite coating formed a mixture of two phases, zinc and cubic Co_5Zn_{21} phases, with smaller crystallite size,

The deposited coating with 20 g/l Cr showed the maximum value of hardness 491,25HV, because of the increase of Cr concentration in the plating bath.

Polarization resistances of Zn-Co composite coating increased with increasing the Cr content.

The data obtained from electrochemical impedance spectroscopy (EIS) assumes that the charge transfer resistance (R_{ct}) is higher and the capacity of the double layer (C_{dl}) decreases value is lower for Zn-Co-Cr composite coating containing 20 g / l Cr alloy compared with those of Zn-Co matrix. This behavior is in good agreement with that obtained from Tafel plot measurements.

Acknowledgements

I would like to thanks "Responsible of Physics Laboratory of Thin Films and Applications (LPCMA)" for their assistance in the preparation of this work.

References

- [1] M. Diafi, K. Degheche, H. B. Temam, *Journal of Fundamental and Applied Sciences***9**, 89 (2017).
- [2] M. Diafi, S. Benramache, E. G. Temam, M. L. Adaika, B. Gasmi, *Acta Metallurgica Slovaca***22**, 171 (2016).
- [3] J. L. O.Aparicio, Y. Measa, G. Trejo, R. Ortega, T.W. Chapman, E. Chainet, P. Ozi, *Electrochimica Acta* **52**, 4742 (2007).
- [4] S.M. Rashwan, A.E. Mohamed, S.M. A.Wahaab, M.M. Kamel, *Journal of Applied Electrochemistry* **33**, 1035 (2003).
- [5] M. Diafi, N. Belhamra, B. T. Hachemi, B. Gasmi, S. Benramache, *Acta Metallurgica Slovaca* **21**, 226 (2015).
- [6] M. Diafi, L. Tahraoui, K. Digheche, F. Khamouli, *Acta Metallurgica Slovaca* **24**, 241 (2018).
- [7] M.S. Chandrasekar, S. Shanmugasigamani, M. Pushpavanam, *Materials Chemistry and Physics* **115**, 603 (2009).
- [8] M. Mouanga, L. Ricq, P. Berçot, *Journal of Applied, Electrochemistry* **38**, 231 (2008)
- [9] I. H. Karahan, *Optoelectron. Adv. Mat.* **2**, 788 (2008).
- [10] T. B. Scherzer, G. Avdeev, T. Vassilev, V.Chakarova, H. Kronberger, M. Monev, *Surface Engineering***35**,1055(2019).
- [11] T. Yang, C.Z. Peng, L. Xiang, H. Cao, *Applied Mechanics and Materials* **456**, 438(2013).
- [12] M. R. E. sharif, Y. J. Su, C. U. Chisholm, A. Watson , *Corrosion Science* **35**, 1259 (1993).
- [13] V. Medeliene, E. Matulionis, *Protection of Metals***38**, 275 (2002).
- [14] V. Chakarova, T.z. B. Scherzer, D. Kovacheva, H. Kronberger, M. Monev, *Corrosion Science* **140**, 73 (2018).
- [15] Z. Zhen, L. Ning, W. C.Qing, L. D. Yu, Z.Y. Ming, W. Gang, *International Journal of Hydrogenenergy* **37**, 13921 (2012).
- [16] S. H. Yeh, C. C. Wan, *Journal of Applied Electrochemistry* **24**, 993 (1994).
- [17] P. Mourya, S. Banerjee, M. Singh, *Corrosion Science***85**, 352 (2014).
- [18] K. Benchekroun, F. Dalard, J. Rameau, *New Journal of Chemistry***26**, 946 (2002).
- [19] M. Moradi, J. Duan, X. Du, *Corrosion Science***69**, 338 (2013).
- [20] E. Cafferty, N. Hackerman, *Journal of The Electrochemical Society***119**, 146 (1972).
- [21] W. Li, Q. He, C. Pei, B. Hou, *Electrochim Acta***52**, 6386 (2007).
- [22] F. Nada, A. Atta, M. Fekry, M. Hamdi, M. Hassaneen, *International Journal of Hydrogen Energy***36**, 6462 (2011).
- [23] A.M.Fekry, M.A. Ameer, *International Journal of Hydrogen Energy***35**, 7641 (2010).
- [24] S. A. E. Meksoud, A. E.Desoky, A. E. Sonbati , A. Belal, R. E. Boz, *International Journal of Scientific Engineering Research*.**4**, 1986 (2013).
- [25] E.M. Sherif, S.M.Park, *Corrosion Science* **48**,4065 (2006).
- [26] N.A. A. Mobarak, K.F. Khaled, M. N.H. Hamed, K. M. A. Azim, *Arabian Journal of Chemistry***4**, 185 (2011).
- [27] N.A. A. Mobarak, K.F. Khaled, M.N.H. Hamed, K.M. A. Azim, N.S. Abdelshafi, *Arabian Journal of Chemistry***3**, 233 (2010).